*Proc. Natl. Acad. Sci. USA*
Vol. 94, pp. 3402–3407, April 1997
Neurobiology

# Patterns of synaptic activity in neural networks recorded by light emission from synaptolucins

**(neurotransmission/exocytosis/optical imaging)**

GERO MIESENBÖCK AND JAMES E. ROTHMAN

Cellular Biochemistry and Biophysics Program, Memorial Sloan–Kettering Cancer Center, 1275 York Avenue, New York, NY 10021

*Contributed by James E. Rothman, December 30, 1996*

**ABSTRACT** **The emission of light, coupled to exocytosis, can in principle be utilized to monitor the activity of a large number of individual synapses simultaneously. To illustrate this concept, fusion proteins of *Cypridina* luciferase and synaptotagmin-I or VAMP-2/synaptobrevin (which we term "synaptolucins") were expressed in cultured hippocampal neurons with the help of viral vectors. Synaptolucins were targeted to synaptic vesicles and, upon exocytosis, formed light-emitting complexes with their cognate luciferin, which was added to the extracellular medium. Photon emissions required a depolarizing stimulus, occurred from regions with high synaptic density as ascertained by vital staining of recycling synaptic vesicles, and were sensitive to $Ca^{2+}$ depletion and clostridial neurotoxins. The method can currently detect exocytosis of the readily releasable pool of synaptic vesicles at a hippocampal synapse, corresponding to about two dozen quanta, but has the potential for greater sensitivity.**

Many problems in neurophysiology can be reduced to questions about the location, timing, and magnitude of synaptic activity, including, for instance, the integration of inputs by a single neuron, synaptic plasticity, and pattern classification and storage by neural networks. The study of these and related problems would greatly benefit from a method that allows direct recording from many synapses simultaneously, with the capacity to reliably detect single exocytotic events. Such a method would appear optimal because, on the one hand, central synapses generally transmit information via the fusion of a single synaptic vesicle (1, 2), while, on the other hand, the computational power of the nervous system arises from networks containing large numbers of synapses (3–5).

While current electrophysiological methods allow the activity of individual synapses to be recorded, they do not permit populations to be studied. There is a practical limit to the number of cells that can be impaled simultaneously with intracellular electrodes, and importantly, an invasive method requires an *a priori* decision on which cells to study, making discovery difficult. Extracellular field recordings with multiple electrodes avoid some of these problems and thereby allow the collective activities of many cells to be measured, but do not permit activity to be ascribed to individual synapses or neurons (6, 7). Optical imaging of light emission from fluorescent indicators of membrane potential or intracellular $Ca^{2+}$ concentration (7–10) greatly increases spatial resolution but again, does not measure synaptic activity directly. An alternative optical approach that offers a direct gauge of synaptic activity is to load synaptic vesicles with fluorescent dyes and to observe dye release (11, 12). However, this method is intrinsically incapable of resolving individual quanta, which can cause only a small decrease in total fluorescence. Despite their limitations, these techniques have opened a window on multicellular phenomena as diverse as the representation of visual scenes by retinal ganglion cells (13) and the emergence of cortical circuits during development (14). Methods that reveal the detailed patterns of synaptic inputs and outputs in entire networks can thus be expected to disclose important new physiological concepts operative at the relatively unexplored interface between cellular and systems neurophysiology.

An ideal method for studying patterns of synaptic activity would consist of an optical signal that reports the act of transmitter release directly, allows detection of every vesicle fusion event, can be regenerated for many rounds of recording, and—less obvious from the above—originates from a genetically encoded probe (i.e., a protein). Genetic control would allow recordings to be obtained from cells, cultures, brain slices, or exposed tissues of transgenic animals, and would afford means to focus on individual neurons (by localized DNA transfer techniques), types of neurons (by cell-type specific promoters), or elements of a circuit (by recombinant viral vectors that spread through synaptic contacts; see ref. 15). We have designed a first generation of such probes, which we term "synaptolucins," and now report their construction and validation.

## MATERIALS AND METHODS

**Synaptolucins.** Total *Cypridina* RNA extracted with Trisolv (Biotecx Laboratories, Houston) served as the template for the reverse transcriptase–PCR synthesis of a cDNA encoding the luciferase (16). The PCR product was subcloned into the amplicon plasmid pα4"a" (17, 18), and its sequence was determined with Sequenase 2.0 (United States Biochemical). To construct synaptolucins-1 and -2, the appropriate portions of the ORFs for *Cypridina* luciferase (16) and, respectively, synaptotagmin-I (19) and VAMP-2/synaptobrevin (20, 21) were fused via stretches of nucleotides encoding the flexible linker -(Ser-Gly-Gly)$_4$-.

The amplicon plasmids were transfected into E5 cells (17, 22) with the help of LipofectAMINE (GIBCO/BRL), and replicated and packaged into virions after infection with 0.1 pfu/cell of the herpes simplex virus (HSV) deletion mutant *d*120 (22). The primary virus stock was passaged on E5 cells until the vector-to-helper ratio exceeded 1:4; the ratio was estimated as the number of synaptolucin-positive Vero cells [by immunostaining, using mAbs M48 (23) and CL69.1 (24)] vs. the number of viral plaques formed after infection of E5 cells.

**PC12 Cells.** PC12 cells were infected at a multiplicity of 1 amplicon virion/cell and at 6 h *p.i.* harvested in buffer H (10 mM Hepes-NaOH, pH 7.4/150 mM NaCl/0.1 mM $MgCl_2$/1 mM EGTA/1 mM phenylmethylsulfonyl fluoride/1 μg/ml each of aprotinin, leupeptin, and pepstatin). Homogenates were prepared by 13 passes through a ball-bearing cell cracker

Abbreviation: HSV, herpes simplex virus.

The publication costs of this article were defrayed in part by page charge payment. This article must therefore be hereby marked "*advertisement*" in accordance with 18 U.S.C. §1734 solely to indicate this fact.


0027-8424/97/943402-6$2.00/0
PNAS is available online at **http://www.pnas.org**.

and postnuclear supernatants (5 min at 5000 × *g*) fractionated on 5–25% (wt/vol) glycerol gradients in a Beckman SW41 rotor, operated for 2 h at 41,000 rpm (25). Gradient fractions were analyzed by SDS/PAGE, Western blotting, and immunostaining.

To measure synaptolucin activities, postnuclear supernatants were solubilized on ice with 1% Nonidet P-40, clarified (10 min at 15,000 × *g*) and diluted 50-fold into buffer L (20 mM Hepes-NaOH, pH 7.4/150 mM NaCl/2 mM $CaCl_2$/2 mM $MgCl_2$) that had been prewarmed to 30°C. After addition of *Cypridina* luciferin to 5 μM, photon fluxes were integrated for 10 sec in an LKB 1250 luminometer calibrated with a [$^{14}$C]hexadecane standard (26). Synaptolucin concentrations were determined by quantitative immunoblotting with mAbs M48 (23) and CL69.1 (24) and [$^{125}$I]protein G (New England Nuclear), using the recombinant cytoplasmic domains of synaptotagmin and VAMP as the standards.

**Hippocampal Neurons.** The hippocampal CA1–CA3 fields of P1 Sprague–Dawley rats were dissected into Earle's balanced salt solution with 10 mM Hepes-NaOH (pH 7.0) and mechanically dissociated after treatment with 20 units/ml papain (Worthington) (27, 28). Cells were plated onto the poly-D-lysine- and laminin-coated surface of 35-mm dishes with central 8-mm glass windows (adhesive substrates were from Sigma). The cultures were maintained in basal medium Eagle with Earle's salts and 25 mM Hepes-NaOH (pH 7.4), supplemented with 20 mM glucose, 1 mM sodium pyruvate, 10% fetal bovine serum, 0.1% Mito+ Serum Extender (Collaborative Biomedical Products, Bedford, MA), 100 units/ml penicillin, 0.1 mg/ml streptomycin, and from day 5 after plating, 5 μM cytosine arabinoside (Sigma) (28). The preparations were infected with HSV amplicon vectors after 1–2 weeks *in vitro*. Viral inocula were diluted to multiplicities of roughly 0.1 in conditioned medium containing 1 mM kynurenate (Fluka), adsorbed for 1 h, removed, and replaced with conditioned medium.

**Optical Recording.** At 8–20 h *p.i.*, culture dishes were transferred to a PDMI-2 microincubator (Medical Systems, Greenvale, NY) mounted on the stage of a Zeiss Axiovert 135 TV microscope and held at 30°C. A Teflon insert forming an 8-mm-wide channel across the optical window was placed in the dish to allow rapid perfusion with either normokalemic solution (25 mM Hepes-NaOH, pH 7.05/119 mM NaCl/2.5 mM KCl/2 mM $CaCl_2$/2 mM $MgCl_2$, 30 mM glucose) or its hyperkalemic counterpart (KCl raised to 90 mM, NaCl reduced to 31.5 mM). Nerve terminals were stained by a 1-min exposure to 3 μM FM 4-64 (Molecular Probes) in hyperkalemic solution (12) with 1% dialyzed bovine serum, followed by superfusion with normokalemic solution for >10 min.

FM 4-64 fluorescence was excited with the 510- to 560-nm band of an attenuated xenon arc lamp; alternatively, synaptolucin bioluminescence was initiated by adding 30 nM luciferin from a 30 μM methanolic stock. Emitted light was collected with a Zeiss ×40/1.3 NA Plan-Neofluar oil immersion objective, 590-nm longpass-filtered in the case of FM 4-64 fluorescence, and focused onto the photocathode of a C2400-30H image intensifier coupled to a C2400-75 charge-coupled device (both from Hamamatsu Photonics, Hamamatsu, Japan). The video signal was 8-bit digitized in an Argus-20 image processor (Hamamatsu Photonics) and saved to a Power Macintosh for analysis, using NIH IMAGE 1.60 (http://rsb.info.nih.gov/nih-image/), TRANSFORM 3.3 (Fortner Research LLC, Sterling, VA), and MATHEMATICA 3.0 (Wolfram Research, Champaign, IL).

## RESULTS AND DISCUSSION

**Synaptolucins.** Synaptolucins are engineered membrane proteins consisting of two modules: a targeting module derived from a synaptic vesicle-specific integral membrane protein, such as synaptotagmin-I (19) or VAMP-2/synaptobrevin (20, 21), and a light-generating module that is constitutively "off" but is switched "on" in the instant of exocytosis. This translates transmitter release into an optical signal. In synaptolucins, the role of the switchable light-generating module is played by a luciferase, attached to the inner surface of synaptic vesicles and acting on a membrane-impermeant substrate. If the substrate is present in the extracellular medium and the enzyme sequestered in synaptic vesicles, light emission cannot occur, but once the vesicle fuses with the presynaptic membrane and the catalytic module is externalized, a burst of photon emission follows. For this strategy to be viable, the luciferase must (*i*) catalyze a sufficiently high photon flux for imaging (a quantity dependent on the enzyme's turnover number and the quantum yield of the light-emitting complex), (*ii*) use a membrane-impermeant substrate, (*iii*) be capable of folding in the endoplasmic reticulum lumen and be targetted to synaptic vesicles, and (*iv*) operate efficiently under the pH and salt conditions of the extracellular environment.

Of the well-characterized bioluminescent systems, that of the ostracod *Cypridina* (or *Vargula*) *hilgendorfii* (29) matches this profile remarkably well, in contrast to the commonly used firefly luciferase, which does not. *Cypridina* luciferase is a monomeric, naturally secreted glycoprotein of 62 kDa (16, 30) that can be expressed in and is secreted from transfected mammalian cells (31); firefly luciferase is peroxisomal. *Cypridina* luciferin (32) carries a guanidino group expected to be positively charged at physiological pH and to thereby render the molecule slowly permeant or even impermeant to membranes. Unlike firefly luciferase, which requires ATP (and, for sustained activity, coenzyme A), *Cypridina* luciferase uses no cofactors other than water and $O_2$ (29). Its luminescent reaction proceeds optimally at pH 7.2 and physiological salt concentrations (30), whereas that of firefly is optimal at low ionic strength (activity is inhibited 5- to 10-fold by physiological salt), alkaline pH, and reducing conditions. With a turnover number of 1600 $min^{-1}$ (33) and a quantum yield of 0.29 (34), *Cypridina* luciferase produces a specific photon flux exceeding that of the optimized firefly system (35) by a factor of at least 50.

We isolated a cDNA encoding *Cypridina* luciferase and constructed two synaptolucins. In synaptolucin-1, the C terminus of luciferase is fused to the N terminus of synaptotagmin-I, located in the lumen of synaptic vesicles. The hybrid protein relies on the cleavable signal peptide encoded by the luciferase gene for membrane translocation and is anchored by the transmembrane domain of synaptotagmin. In synaptolucin-2, the mature N terminus of luciferase is fused to the C terminus of VAMP-2, located in the vesicle lumen. This results in a type II hybrid protein with a membrane-anchor segment that also serves as a noncleavable signal sequence. The luciferase cDNA we obtained (GenBank accession no. U89490) differed from the published DNA sequence (16) at 30 positions, only three of which gave rise to amino acid substitutions: Asp-16 → Val, Ile-346 → Leu, and Asn-495 → Ser. The first substitution shifted the predicted signal peptide cleavage site (16), leading us to consider Gln-19 the mature N terminus and to construct synaptolucin-2 accordingly.

When expressed in PC12 cells, the synaptolucin genes directed the synthesis of membrane proteins of the expected sizes which cosedimented with their respective targeting modules in velocity gradients (Fig. 1). The synaptolucins, like VAMP and synaptotagmin, were found both in synaptic vesicles (fractions 4–9) and endosomes (fractions 11–14) (25). Both synaptolucins were enzymatically active, with a $k_{cat}$ of 5.2 and 3.7 photon emissions $sec^{-1}$ per synaptolucin-1 and -2 molecule, respectively, determined as described in *Materials and Methods*.

**Imaging Neurotransmitter Release.** Initial experiments on hippocampal neurons, performed at a saturating luciferin

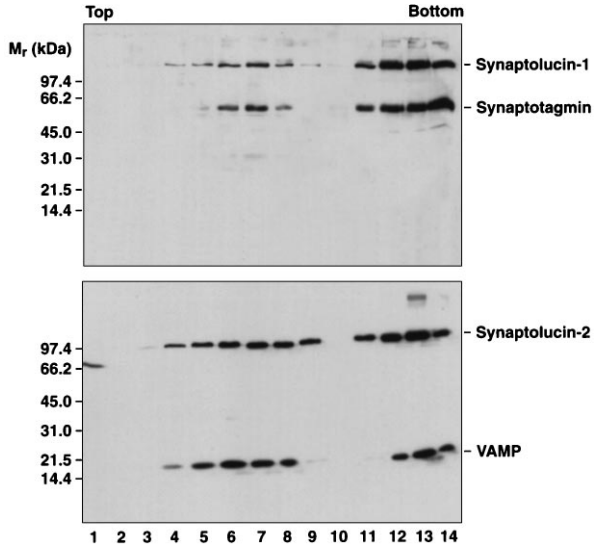


FIG. 1. Cofractionation of synaptolucins with synaptic vesicle proteins. Amplicon-infected PC12 cells were homogenized and postnuclear supernatants sedimented into 5–25% glycerol gradients. Small synaptic vesicles band in fractions 4–9, endosomes in fractions 11–14 (25). The bottom fraction contains material collected on a sucrose cushion; compared with the slower-sedimenting fractions, only 15% of this material was analyzed by SDS/PAGE. Proteins were precipitated with trichloroacetic acid, separated on 8–18% gels, and transferred to nitrocellulose. The filters were probed with mAb M48 (23), directed against synaptotagmin-I (*Top*), or mAb CL69.1 (24), directed against VAMP-2 (*Bottom*). Bound antibodies were visualized by ECL (Amersham).

concentration of 5 $\mu$M (30), revealed an unexpected problem: a depolarizing stimulus was not required for photon emissions to occur. We suspected that this signal arose from the intracellular synaptolucin pool, which would become visible if *Cypridina* luciferin, an imidazo[1,2-a]pyrazine nucleus with mostly hydrophobic substitutions (32), crossed biological membranes once its guanidino group was deprotonated. We thus lowered the pH of our bath solutions from 7.4 to 7.05 to favor the protonated luciferin species, and decreased their luciferin content to reduce diffusion across membranes. Indeed, at a luciferin concentration of 30 nM, the background signal disappeared and photon emissions became stimulation-dependent. However, longer photon-counting times were required because at a luciferin concentration so far below the $K_m$ of luciferase (0.52 $\mu$M; ref. 30), synaptolucin operated at only 3% of its $V_{max}$.

Fig. 2 illustrates a typical imaging experiment on hippocampal neurons infected with an HSV amplicon vector transducing synaptolucin-1. We first obtained a map of the synapses within the field of view (Fig. 2*A*) by taking the preparation through a depolarization cycle (12) in the presence of FM 4-64 (36), a member of the family of fluorescent dyes that are known to stain recycling synaptic vesicles (11). FM 4-64 was chosen over the more widely used FM 1-43 (11, 12) because it does not absorb significantly at 462 nm, the emission wavelength of *Cypridina* luciferin (34), and thus permits the acquisition of an unperturbed synaptolucin signal from a stained preparation. After perfusion with normokalemic solution for at least 10 min, sufficient to replenish the synaptic vesicle pool and to remove excess FM 4-64, we added a bolus of luciferin to the bath solution and counted photon emissions for the next 30 sec. In many cases, such as the one shown in Fig. 2*B*, some photons were registered in the absence of a depolarizing stimulus, but these originated mainly from regions without an appreciable density of synapses (compare the areas marked by dashed red lines in Fig. 2 *A* and *B*). It is likely that HSV-infected glial cells in the mixed culture are the source of this background signal,

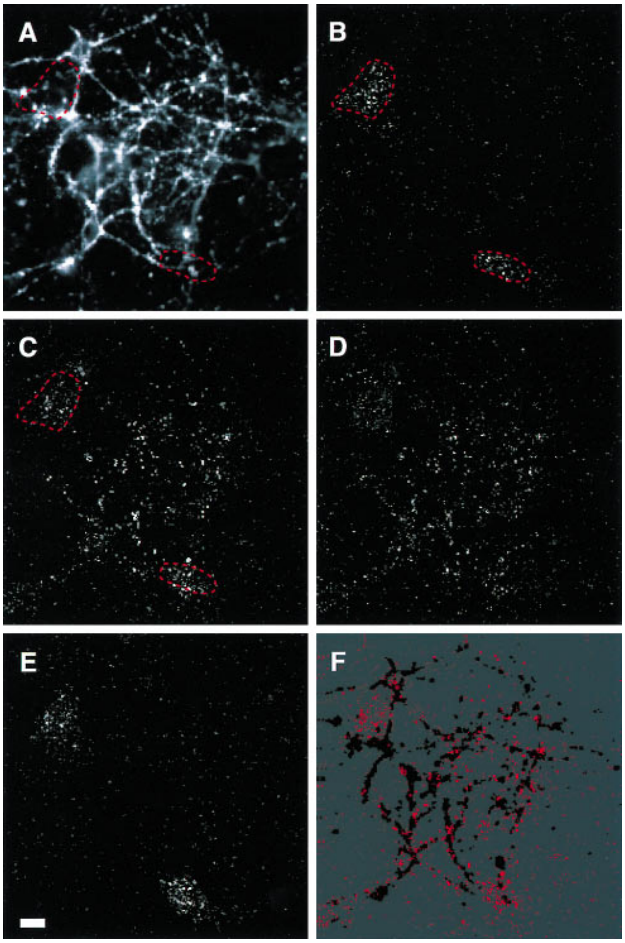


FIG. 2. Hippocampal neurons expressing synaptolucin-1, imaged by wide-field microscopy. About 60% of the neurons were infected by HSV transducing synaptolucin-1. (*A*) The synaptic map, revealed by loading nerve terminals with FM 4-64. The fluorescent signal from FM 4-64 was acquired at low intensifier gain and averaged over 32 video frames. (*B–E*) Photon registrations accumulated from synaptolucin emissions over 30 sec, obtained at 30 nM luciferin, maximum image intensifier gain, and a discriminator value for photon detection that suppressed background and equipment noise (photon counts in the presence of a depolarizing stimulus but the absence of luciferin) to an average of 1.06 photon registrations per 100-pixel field. The preparation was imaged successively in normokalemic solution (*B*) and during three hyperkalemic challenges to induce exocytosis, performed in either the presence (*C* and *D*) or the absence (*E*) of external $Ca^{2+}$. Ten minutes under resting conditions elapsed between each of the successive stimuli. The dashed red lines in *A–C* mark areas of stimulation-independent synaptolucin activity, in all likelihood due to virus-infected glial cells. (*F*) Superimposition of the synaptolucin signal of *C*, colored here in red, onto a binary version of the synaptic map. The binary map was constructed by thresholding *A* such that pixels with an intensity above the 97th percentile appear in black. (Bar = 20 $\mu$m.)

because the neurotropism of HSV in hippocampal cultures is incomplete (17), and because synaptotagmin, the targeting module of synaptolucin-1, appears at the cell surface when expressed in nonneuronal cells (37). This problem could be circumvented by using neuron-specific promoters.

To record light emission resulting from synaptic activation, the preparation was perfused with hyperkalemic solution to depolarize the neurons, open voltage-gated $Ca^{2+}$ channels in presynaptic terminals, and trigger exocytosis. Because *Cypridina* luciferin is unstable in aqueous solution, decomposing with a $t_{1/2}$ on the order of 1 min (29, 30), a second bolus of luciferin was added immediately after depolarization, and photons were counted for 30 sec thereafter. A far greater number of photons were registered than in the absence of a

stimulus, and now their pattern (Fig. 2*C*) was similar to the synaptic map recorded with FM 4-64 (Fig. 2*A*). The match, however, was imperfect, presumably because the synaptolucin image contained background emissions from virus-infected glial cells (compare the areas marked by dashed red lines in Fig. 2 *B* and *C*), and because only a subset of synapses (those formed by neurons that are virus-infected) are potential light sources. Repeating the depolarization after a 10-min resting period evoked a similar but not entirely identical response (Fig. 2*D*), whereas depolarization without $Ca^{2+}$ influx (by omitting free $Ca^{2+}$ from the hyperkalemic solution) left the photon count at baseline level, with photon emissions only from the regions attributed to glial cells (compare Fig. 2 *E* and *B*).

To examine the degree of correspondence between the sites of synaptolucin activity and the synaptic map more rigorously, we overlaid, as depicted schematically in Fig. 2*F*, photon-counting images with a binary filter constructed from the synaptic map (Fig. 2*A*). The filter was chosen such that it "transmitted" only at pixels where the intensity of FM 4-64 fluorescence exceeded the 97th percentile of the grayscale (black areas in Fig. 2*F*) but blocked transmission elsewhere (gray areas in Fig. 2*F*). If such a digital filter scans another image and the intensity of the transmitted signal is plotted as a function of the relative shift between filter and image, maxima occur where the filter detects a matching structure in the image (38). Fig. 3 shows the result of scanning two synaptolucin images, Fig. 2 *B* and *C*, with a filter constructed from Fig. 2*A*. Clearly, the signal in Fig. 2*B* has no counterpart in the synaptic map, supporting its identification as a contaminant of nonneuronal origin (Fig. 3 *Lower*). The sites of evoked photon emissions in Fig. 2*C*, by contrast, produce a sharp maximum where filter and image are in register and thus map to nerve terminals (Fig. 3 *Upper*).

In addition to characteristic sensitivities to membrane potential and extracellular $Ca^{2+}$, an optical signal generated by synaptic vesicle exocytosis should be susceptible to clostridial neurotoxins that inactivate components of the machinery for transmitter release (39). Fig. 4 shows an experiment performed to address this point. An FM 4-64/synaptolucin image pair was first acquired to locate synaptolucin-expressing synapses (Fig. 4*A*). Following a second round of FM 4-64 loading (to compensate for dye release during acquisition of the synaptolucin image, see Fig. 4*B*), the preparation was incubated on the microscope stage with 20 nM each of botulinum neurotoxin serotypes B and F (39) plus 1 $\mu$M tetrodotoxin to suppress action potentials (and hence, dye release) during the incubation. After 3 h of toxin treatment a second pair of images was recorded, and noted to differ from the first in two respects: (*i*) the dimming of FM 4-64 fluorescence that originally accompanied the hyperkalemic challenge now failed to occur, indicating that exocytosis was effectively blocked (compare Fig. 4 *B* and *D*), and (*ii*) photon emissions from synaptolucin disappeared concomitantly (compare Fig. 4 *A* and *C*). This ties the synaptolucin signal firmly to the process of neurotransmitter release.

**Potential Applications and Current Limitations.** The reproducible pattern of photon registrations in repeated trials (compare Fig. 2 *C* and *D*) attests to the reliability of synaptolucins as indicators of exocytosis, with many possible applications. For example, the interpretation of many studies on synaptic plasticity is fraught with controversy, possibly because the pre- and postsynaptic components of neurotransmission cannot be distinguished by traditional methods, which are all indirect (40). Measuring exocytosis directly via synaptolucins, before and after maneuvers that alter synaptic strength, could help to resolve ambiguities. Or, the multiple inputs to a postsynaptic neuron could be mapped with the help of synaptolucins. If the postsynaptic neuron's membrane potential is monitored electrically, the shape of a synaptic potential as it arrives after propagation through the dendritic tree could be measured and immediately correlated with its anatomical site

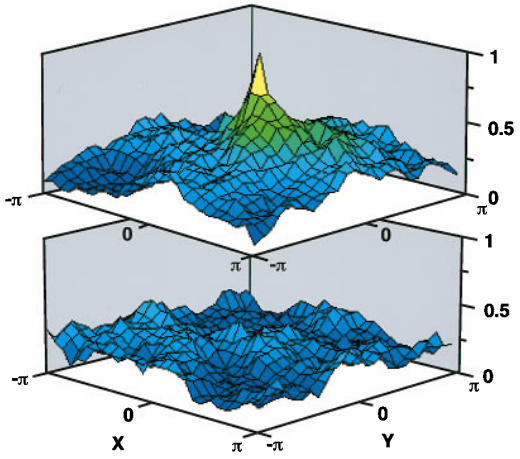


FIG. 3. Matched filtering of two synaptolucin images, Fig. 2 *B* (control) and *C* (exocytosis triggered), with their common synaptic map, Fig. 2*A*, as shown schematically in Fig. 2*F*. The *x*- and *y*-axes indicate the relative shifts between filter and image in these projections, and the ordinate the normalized cross-correlation function, a measure of the match between image and filter (38). The function is computed by pointwise multiplication in the spatial frequency domain and, due to the properties of the Fourier transform, periodic (38). Only a single period, from $-\pi$ to $\pi$ in the *x*- and *y*-directions, is shown. At shift (0,0), filter and image are in register, at shifts $(x,\pm\pi)$ or $(\pm\pi,y)$, the filter's center is displaced to an edge of the image. (*Upper*) Scanning of Fig. 2*C*, showing evoked synaptolucin emissions. Note the peak at a filter shift of (0,0), indicating a matching structure in the image. (*Lower*) Scanning of Fig. 2*B*, lacking evoked synaptolucin emissions. Note the absence of a central peak.

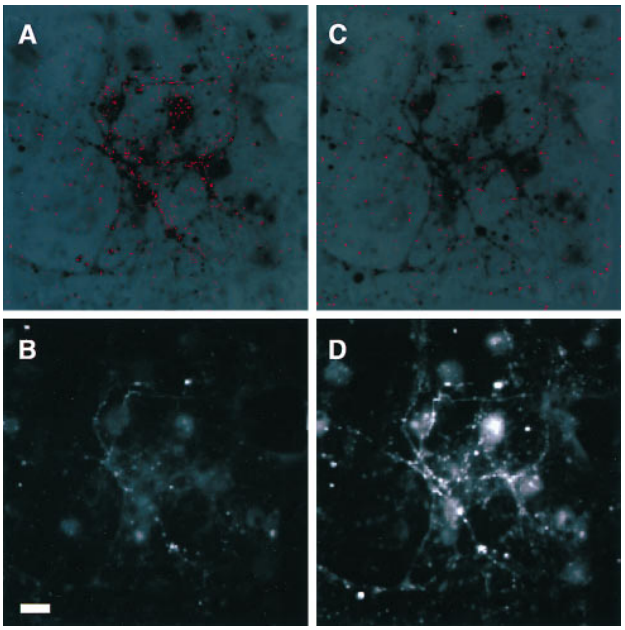


FIG. 4. Hippocampal neurons expressing synaptolucin-1, imaged by wide-field microscopy at the same intensifier and detector settings as in Fig. 2. (*Upper*) Photon registrations from synaptolucin emissions during the first 30 sec after triggering exocytosis, colored in red and superimposed on synaptic maps obtained with FM 4-64. (*Lower*) FM 4-64 images after a 30-sec hyperkalemic challenge. *A* and *B* were recorded before and *C* and *D* after treatment with botulinum neurotoxins B and F. Botulinum neurotoxins were applied during a 5-min depolarization (to enhance toxin uptake into recycling synaptic vesicles) and then during a 3-h incubation in complete medium with 1 $\mu$M tetrodotoxin. Note the marked decrease in FM 4-64 fluorescence intensity in *B* as opposed to *D*. (Bar = 20 $\mu$m.)

Table 1. Vesicle fusion events at single synapses

| Method of estimation | No. of fusion events | Photons emitted per vesicle | Photon emission rate per vesicle, $sec^{-1}$ |
|---|---|---|---|
| Kinetics of transmitter release | 67 | 4.7 | 0.38 |
| Photon count fluctuations | 51 | 6.1 | 0.49 |

Synaptic vesicle exocytosis and recycling were modeled as Poisson processes (1, 2, 41, 42), using kinetic parameters obtained in studies of transmitter or dye release from identified synapses of hippocampal neurons in culture (12, 43, 44). This stochastic model provided the basis for estimating the number of fusion events, either on the assumption of a fixed number of statistically independent release sites per synapse (41–43), or through an analysis of photon count fluctuations (45, 46), using the data displayed in Table 2. (The mathematical details are available by e-mail from g-miesenboeck@ski.mskcc.org.)

of origin, with important implications for input integration (5). The pattern of activation of individual synaptic inputs could be measured in relation to the activation of a postsynaptic neuron, affording a direct means of establishing firing rules.

Does current synaptolucin technology allow for these applications, each of which would require the ability to detect light emitted from the fusion of a single synaptic vesicle? The sensitivity and temporal resolution afforded by synaptolucins are determined by three factors: the number of synaptolucin molecules per vesicle, their specific emission rate, and the time over which photon counts can be integrated to keep pace with the relevant physiology. At video rates, this interval is usually a single video frame, or about 30 msec. At the other extreme, with long photon-counting times as in the present experiments, the timing of the synaptic vesicle cycle itself becomes limiting. In such cases, photon emission begins as a vesicle fuses with the presynaptic membrane, probabilistically (41, 42) at any time during the observation period, and ends as its synaptolucins are re-internalized, again probabilistically, or the camera shutter is closed. Vesicle recycling will terminate synaptolucin activity virtually instantaneously: if luciferin is taken up by recycling vesicles at its bulk concentration of 30 nM, only about 1 in a 1000 recycled vesicles will contain a luciferin molecule (as can be calculated from the internal diameter of a synaptic vesicle of 50 nm), and those few that do will consume the internalized luciferin (via luciferase) rapidly. This effectively prevents the visualization of endocytosed vesicles and limits photon emissions to the synaptolucin's dwell time in the presynaptic membrane.

Estimates for the number of quanta released under our experimental conditions and for the average observation time per synaptolucin can be derived by modelling vesicle release and recycling as Poisson processes (1, 2, 41, 42). At a typical hippocampal synapse, the probability for exocytosis drops from an initial rate of about 20 quanta $sec^{-1}$ (the "readily releasable pool") to a basal rate of 2 quanta $sec^{-1}$ (43); the transition between initial and basal release rates occurs exponentially with a time constant of 1.2 sec (43). The probability of recycling is assumed constant throughout, with a $t_{1/2}$ of 20 sec (12, 44). When such a synapse is observed for 30 sec under maintained hyperkalemic stimulation, an average of 67 quantal releases will take place (Table 1), and the synaptolucins contained in one quantum (i.e., one vesicle) will emit for an average of 13 sec (see the legend to Table 1). Under the same conditions, an average of 12 photon registrations were counted per synapse (Table 2). Correcting for the detection efficiency (see Table 2), this translates into about 310 photon emissions for the entire synapse, 4.7 photon emissions for a single vesicle, and a photon emission rate of 0.38 $sec^{-1}$ per vesicle (Table 1), equalling that generated by about three synaptolucin molecules *in vitro* at the same limiting luciferin concentration of 30 nM.

A fluctuation analysis (45, 46) of the photon counts in Table 2, obtained from the experiment shown in Fig. 2*C*, estimates the number of released quanta as 51 per synapse and the photon emission rate as 0.49 $sec^{-1}$ per vesicle, in rather close agreement with the values derived from kinetic arguments alone (Table 1).

Comparing the number of photon registrations (about 12 per synapse) with the actual number of vesicle fusion events (about 60 per synapse) indicates that the majority of fusion events remained undetected with present technology. With a photon emission rate of 0.4–0.5 $sec^{-1}$ per vesicle (Table 1) and an overall photon detection efficiency of about 4% (Table 2), the time between two successive photon registrations from synaptolucins originating in the same vesicle (the waiting time for the stochastic process) would average about 50 sec. This is considerably longer than the average 13 sec for which a synaptolucin was observed. Hence under our present conditions, synaptolucins will often be re-internalized before a single photon emission can be detected, and those vesicle fusion events that do register cannot be precisely located on a temporal scale.

**Future Prospects.** Initial experiments with synaptolucins have established the feasibility of a potentially important new principle for functional analysis of neural networks—the coupling of light emission to synaptic vesicle exocytosis to provide a direct optical image of synaptic activity. However, while it has been shown that synaptolucins can faithfully record the averaged properties of many vesicle fusion events, the present sensitivity is too low for the detection of single exocytotic events.

Improvements that should allow synaptolucins to perform at the level of single quanta, with increased reliability and better temporal resolution, can be readily envisaged. First, we now must employ luciferin at subsaturating concentrations to minimize its penetration into cells, limiting luciferase to about 3% of its maximum velocity. Use of a truly membrane impermeant luciferin derivative at saturating concentrations would increase photon emissions about 35-fold. Second, there are currently only about three light-generating modules per synaptic vesicle in the HSV-infected neurons. This number could be increased (*i*) by gene replacement technology to fully substitute synaptolucins for VAMP and/or synaptotagmin and (*ii*) by including multiple light-generating modules in a single synaptolucin. Singly,

Table 2. Photon counts

| Photon counts per field | Efficiency | | | Photons emitted per field |
|---|---|---|---|---|
| | Collection | Detection | Overall | |
| 12 ± 3.9 | 0.29 | 0.13 | 0.04 | 310 |

The gray-level increment corresponding to a single photon count was determined from the histogram of Fig. 2*C*, and the number of photon registrations over a 30-sec period counted in fifty 2 × 2-pixel fields, corresponding to 1.8 × 1.8-$\mu$m areas in the specimen plane. These fields were selected by two criteria: (*i*) FM 4-64 fluorescence in excess of the 97th percentile (see Fig. 2*F*), and (*ii*) a >5-fold increase in synaptolucin activity upon depolarization. To convert photon counts to photon emissions, two correction factors were used: the collection efficiency of a 1.3 NA oil immersion objective, defined as the fraction of photons emitted from the focal plane that fall into the objective's acceptance cone, and the detection efficiency of the intensifier photocathode (C2400-30H; Hamamatsu Photonics) at 462 nm.

or in combination, these engineering steps should permit reliable detection of single vesicle fusion events at every visible synapse.

We are greatly indebted to Dr. Osamu Shimomura for his generosity in providing *Cypridina* luciferin. We also thank Dr. Yoshiaki Toya for the *Cypridina*, Dr. Dora Ho for pα4"a", Dr. Neal DeLuca for E5 cells and HSV strain *d*120, Dr. Giampietro Schiavo for botulinum neurotoxins, and Dr. Qais Al-Awqati for his thoughtful comments on the manuscript. This work was supported by the Mathers Charitable Foundation and by postdoctoral fellowships from the Austrian Fonds zur Förderung der wissenschaftlichen Forschung and the Charles H. Revson and Charles A. Dana Foundations.

1. Redman, S. (1990) *Physiol. Rev.* **70,** 165–198.
2. Stevens, C. F. & Wang, Y. (1995) *Neuron* **14,** 795–802.
3. Anderson, J. A. & Rosenfeld, E., eds. (1988) *Neurocomputing* (MIT Press, Cambridge, MA).
4. Shepherd, G. M., ed. (1990) *The Synaptic Organization of the Brain* (Oxford Univ. Press, Oxford), 3rd Ed.
5. McKenna, T., Davis, J. & Zornetzer, S. E., eds. (1992) *Single Neuron Computation* (Academic, Boston).
6. Meister, M., Pine, J. & Baylor D. A. (1994) *J. Neurosci. Methods* **51,** 95–106.
7. Stenger, D. A. & McKenna, T. M., eds. (1994) *Enabling Technologies for Cultured Neural Networks* (Academic, San Diego).
8. Grinvald, A. (1985) *Annu. Rev. Neurosci.* **8,** 263–305.
9. Tsien, R. Y. (1989) *Annu. Rev. Neurosci.* **12,** 227–253.
10. Tsien, R. Y. & Waggoner, A. (1995) in *Handbook of Biological Confocal Microscopy*, ed. Pawley, J. B. (Plenum, New York), 2nd Ed., pp. 267–279.
11. Betz, W. J. & Bewick, G. S. (1992) *Science* **255,** 200–203.
12. Ryan, T. A., Reuter, H., Wendland, B., Schweizer, F., Tsien, R. W. & Smith, S. J. (1993) *Neuron* **11,** 713–724.
13. Meister, M. (1996) *Proc. Natl. Acad. Sci. USA* **93,** 609–614.
14. Katz, L. C. & Shatz, C. J. (1996) *Science* **274,** 1133–1138.
15. Kuypers, H. G. J. M. & Ugolini, G. (1990) *Trends Neurosci.* **13,** 71–75.
16. Thompson, E. M., Nagata, S. & Tsuji, F. I. (1989) *Proc. Natl. Acad. Sci. USA* **86,** 6567–6571.
17. Ho, D. Y. (1994) *Methods Cell Biol.* **43,** 191–210.
18. Lawrence, M. S., Ho, D. Y., Dash, R. & Sapolsky, R. M. (1995) *Proc. Natl. Acad. Sci. USA* **92,** 7247–7251.
19. Perin, M. S., Fried, V. A., Mignery, G. A., Jahn, R. & Südhof, T. C. (1990) *Nature (London)* **345,** 260–263.
20. Elferink, L. A., Trimble, W. S. & Scheller, R. H. (1989) *J. Biol. Chem.* **264,** 11061–11064.
21. Südhof, T. C., Baumert, M., Perin, M. S. & Jahn, R. (1989) *Neuron* **2,** 1475–1481.
22. DeLuca, N. A., McCarthy, A. M. & Schaffer, P. A. (1984) *J. Virol.* **56,** 558–570.
23. Matthew, W. D., Tsavaler, L. & Reichardt, L. F. (1981) *J. Cell Biol.* **91,** 257–269.
24. Edelmann, L., Hanson, P. I., Chapman, E. R. & Jahn, R. (1995) *EMBO J.* **14,** 224–231.
25. Clift-O'Grady, L., Linstedt, A. D., Lowe, A. W., Grote, E. & Kelly, R. B. (1990) *J. Cell Biol.* **110,** 1693–1703.
26. Hastings, J. W. & Weber, G. (1963) *J. Opt. Soc. Am.* **53,** 1410–1415.
27. Huettner, W. J. & Baughman, R. W. (1986) *J. Neurosci.* **6,** 3044–3060.
28. Geppert, M., Goda, Y., Hammer, R. E., Li, C., Rosahl, T. W., Stevens, C. F. & Südhof, T. C. (1994) *Cell* **79,** 717–727.
29. Johnson, F. H. & Shimomura, O. (1978) *Methods Enzymol.* **57,** 331–364.
30. Shimomura, O., Johnson, F. H. & Saiga, Y. (1961) *J. Cell. Comp. Physiol.* **58,** 113–124.
31. Inouye, S., Ohmiya, Y., Toya, Y. & Tsuji, F. J. (1992) *Proc. Natl. Acad. Sci. USA* **89,** 9584–9587.
32. Kishi, Y., Goto, T., Hirata, Y., Shimomura, O. & Johnson, F. H. (1966) *Tetrahedron Lett.* **29,** 3427–3436.
33. Shimomura, O., Johnson, F. H. & Masugi, T. (1969) *Science* **164,** 1299–1300.
34. Shimomura, O. & Johnson, F. H. (1970) *Photochem. Photobiol.* **12,** 291–295.
35. Wulff, K. (1981) in *Bioluminescence and Chemiluminescence*, eds. DeLuca, M. A. & McElroy, W. D. (Academic, New York), p. 219.
36. Henkel, A. W. & Betz, W. J. (1995) *J. Neurosci.* **15,** 8246–8258.
37. Feany, M. B., Yee, A. G., Delvy M. L. & Buckley, K. M. (1993) *J. Cell Biol.* **123,** 575–584.
38. Duda, R. O. & Hart, P. E. (1973) *Pattern Classification and Scene Analysis* (Wiley, New York).
39. Montecucco, C. & Schiavo, G. (1995) *Q. Rev. Biophys.* **28,** 423–472.
40. Bliss, T. V. P. & Collingridge, G. L. (1993) *Nature (London)* **361,** 31–39.
41. Katz, B. (1969) *The Release of Neural Transmitter Substances* (Liverpool Univ. Press, Liverpool, U.K.).
42. Bekkers, J. M. & Stevens, C. F. (1995) *J. Neurophysiol.* **73,** 1145–1156.
43. Stevens, C. F. & Tsujimoto, T. (1995) *Proc. Natl. Acad. Sci. USA* **92,** 846–849.
44. Ryan, T. A., Smith, S. J. & Reuter, H. (1996) *Proc. Natl. Acad. Sci. USA* **93,** 5567–5571.
45. Katz, B. & Miledi, R. (1972) *J. Physiol. (London)* **224,** 665–699.
46. Neher, E. & Stevens, C. F. (1977) *Annu. Rev. Biophys. Bioeng.* **6,** 345–381.